

# Atomic structure of highly ordered pyrolytic graphite doped with boron

Eunkyung Kim, Ilwhan Oh, Juhyoun Kwak \*

*Department of Chemistry, Korea Advanced Institute of Science and Technology (KAIST), 373-1 Kusong-dong, Yuseong-gu, Taejeon 305-701, Republic of Korea*

Received 20 July 2001; received in revised form 3 September 2001; accepted 3 September 2001

## Abstract

Boron-doped carbon was prepared by the high-temperature reaction of  $B_2O_3$  with the highly ordered pyrolytic graphite (HOPG). In order to reveal the effect of the boron doping on the HOPG structure, several experimental tools were employed such as X-ray photoelectron spectroscopy (XPS), X-ray diffraction (XRD), scanning tunneling microscopy (STM), and atomic force microscopy (AFM). While the interlayer spacing of the graphite plane remains virtually unchanged, the boron doping makes the graphite plane of HOPG more disordered. Both the STM and the AFM studies show that the boron-doped HOPG surface is deformed not only in its bonding geometry, but also in its electronic structure. The overall results imply that the boron atom is substituted for the carbon atom rather than is intercalated into the graphite layers. © 2001 Elsevier Science B.V. All rights reserved.

**Keywords:** Boron-doped carbon; Scanning tunneling microscopy (STM); Atomic force microscopy (AFM); X-ray photoelectron spectroscopy (XPS); X-ray diffraction (XRD)

## 1. Introduction

A lot of attention has been paid to the boron-doped carbon materials due to not only the interesting fundamental aspects such as their electronic and structural properties, but also the plausible application such as a high-temperature oxidation protection for carbon composites and as an anode material for Li-ion batteries. Several research groups [1–7] showed that the boron atom could substitute for the carbon atom in the graphite structure and promote the graphitization of pyrolytic graphite. It has been also reported that boron-substituted carbons showed greater reversible capacities and enhanced anode performance because the doped boron acts as electron acceptor and therefore alters the electronic properties without any large distortion of the crystal lattice [1,9,20].

Lowell [10] previously reported that the boron-substituted graphite could be prepared by heating the graphite with  $B_4C$  at high temperature with the maximum boron content being 2.35 at.%. Recently, there have

been numerous reports [1–9] on the substitutional boron synthesis using with the chemical vapor deposition (CVD) method, which can systemically control the amount of substituted boron. Furthermore, the technique has contributed to the various studies for characterizing the boron-doped carbons. For example, Way et al. [11] conducted a detailed characterization of a series of systematically prepared samples dependent on the boron concentration using X-ray diffraction (XRD), auger electron spectroscopy (AES), and X-ray absorption spectroscopy (XAS). Additionally, Endo and co-workers [1,6–8] investigated that the electrochemical properties of the boron-doped graphitized materials depend on the structural geometry and chemical composition of the carbon materials. Consequently, it was shown that Li is intercalated at higher potential and the cycle efficiency is improved in the B-doped carbons [9,11–13].

Although much effort has been put into the characterization of the boron-doped graphite, there is still limited information on its structure [14,15]. In this paper, we employed several structure-sensitive experimental tools to investigate the structure of the boron-doped highly ordered pyrolytic graphite (HOPG). The effect of the boron doping on the atomic structure of HOPG would be discussed in terms of the boron-doping mode.

\* Corresponding author. Tel.: +82-42-869-2833; fax: +82-42-869-2810.

E-mail address: jhkwak@cais.kaist.ac.kr (J. Kwak).

## 2. Experimental

### 2.1. Sample preparation

HOPG (Structure Probe, PA) was freshly prepared by cleaving with an adhesive tape. Boron doping was accomplished by mixing HOPG with 10 wt%  $B_2O_3$  particles and then heat-treatment in the furnace under the high purity of Ar gas (99.999%) to 2600 °C for 1 hr [21].

### 2.2. Characterization of the boron-doped HOPG

Surface analysis by XPS (Thermo VG Microtech, UK) was performed by irradiating the sample with Mg  $K_{\alpha}$  X-ray (1253.6 eV). The boron content was roughly estimated to be 5 wt% by the analysis of XPS signal, which might involve the experimental errors [22]. An XRD measurement was done with a synchrotron radiation at the beamline 3C2 of the pohang light source (PLS).

STM images were obtained in constant current mode with Topometrix TMX2000. An electrochemically etched Pt/Ir wire (Molecular Imaging, AR) was used as the STM tip. Atomic force microscopy (AFM) experiments were conducted in contact mode using a V-shaped silicon nitride cantilever (Topometrix, CA). All images are presented unfiltered.

## 3. Results and discussion

In order to confirm the presence of the doped B in the carbon structure and to estimate the electronic effect of the doping, the XPS measurement is performed. Fig. 1 shows the XPS of the HOPG with and without B doping. The C 1s peak for the B-doped HOPG at 284.4 eV appears at slightly lower binding energy than that of the pure HOPG at 284.6 eV (Fig. 1(a)). This minute but detectable shift is probably related to the lowered  $\pi$  electron density in the B-doped HOPG, which might be caused by the chemical bonding of C atoms with the electron deficient B atom. The lowering of the binding energy with the B doping was also observed in the previous reports [1,7]. We also note that the C 1s peak becomes slightly wider upon B doping, which might result from the structural disorder induced by the B doping, as will be discussed in more detail in the following.

Fig. 1(b) shows the B 1s peak for the B-doped HOPG at about 188 eV, whereas the pure HOPG shows no peak. Several kinds of boron compounds can contribute to the XPS response. It was proposed that the B cluster gives rise to the component at 186.5 eV, the B atom connected to other B as  $B_4C$  at 187.6 eV, and the B atom substituted into the carbon structure at 188.8 eV [3–5].

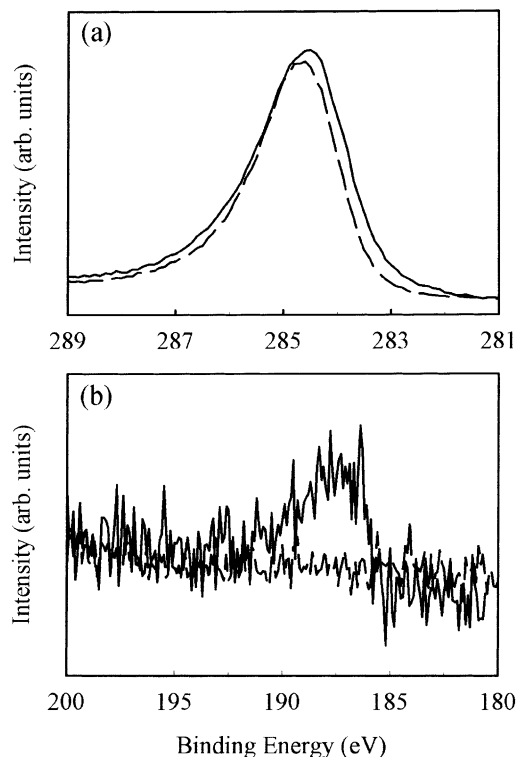


Fig. 1. (a) XPS C 1s spectra and (b) B 1s spectra of HOPG (dashed line) and B-doped HOPG (solid line).

Fig. 2 presents the XRD for the B-doped and the undoped samples of HOPG. For the undoped HOPG, a strong peak is observed at  $26.495^\circ$ , which is the diffraction from the 002 planes. With the B doping, the full width at half maximum (FWHM) of the XRD peak for the B-doped HOPG ( $0.087^\circ$ ) increases as compared to that of the undoped HOPG ( $0.067^\circ$ ). It is also observed that 004 and 006 lines show the similar tendency. This indicates that the B doping gives more disorder to the 002 planes of the HOPG because the

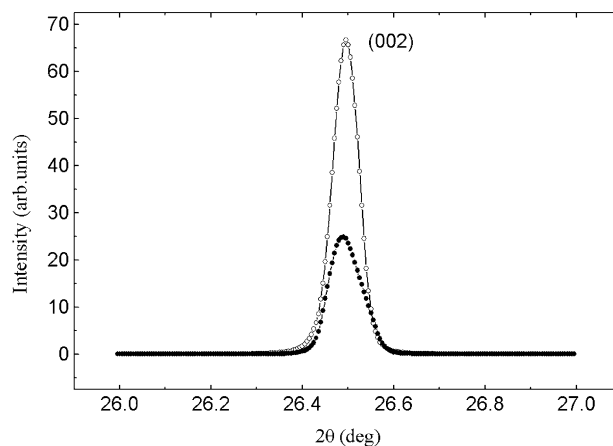


Fig. 2. XRD pattern of HOPG (open circle) and B-doped HOPG (closed circle).

FWHM value of the XRD peak has a direct relevance to the crystallinity of the sample [16]. This is in contrast to the previous results [1,3–6] that the B substitution improves the crystallinity of carbon material. The discrepancy might be attributed to the different kind of carbons investigated.

Generally, the B-doped graphite shows the smaller  $d_{002}$  values than the pure graphite [6,11]. It is related to the depleted  $\pi$  electron density between the graphite planes, which would lead to shorter interlayer distance [6]. In our XRD measurements, however, the B doping makes the interlayer spacing of the HOPG virtually unchanged. It seems that the B doping has little effect to the interlayer spacing of the well-ordered pure carbons such as HOPG, relative to that of the disordered graphite.

In order to visualize the effect of the B doping on the surface structure of the HOPG, scanning probe mea-

surements are performed. Fig. 3(a) shows the STM image of the B-doped HOPG, while in Fig. 3(b) is shown the atomically resolved STM image of the undoped HOPG for comparison. After the B doping, several defects appear as randomly dispersed hillocks on the originally flat surface, with their diameter varying from a few angstroms to several tens of angstroms. As mentioned above, the B atom is likely to substitute into the graphite layer, reducing the  $\pi$  electron density and lowering the Fermi level. Consequently, this probably induces the local distortion in both the topographic and the electronic structures of HOPG. It is unlikely that the hillock feature corresponds to the B atom physisorbed on the basal plane because it is observed even after cleaving the sample with an adhesive tape.

Fig. 4(a) shows the AFM image of the B-doped HOPG, while in Fig. 4(b) is shown the atomically resolved AFM image of the undoped HOPG for com-

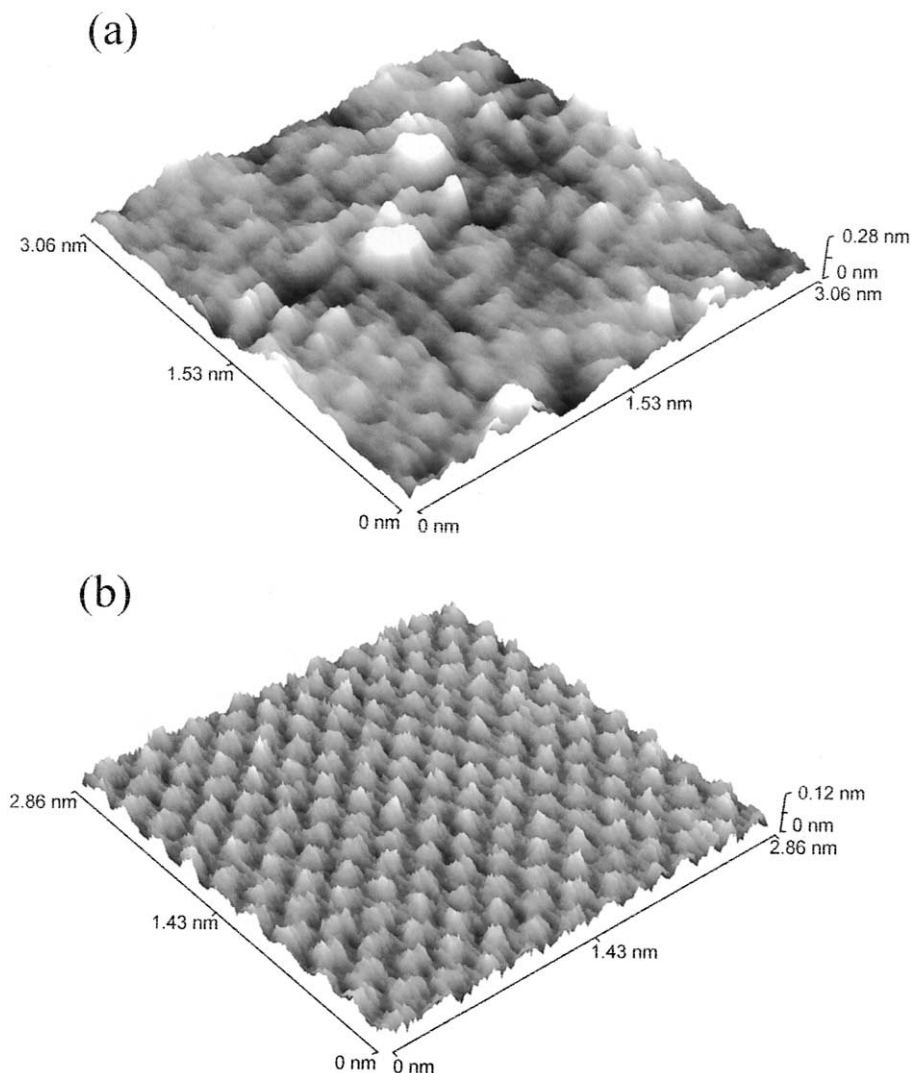


Fig. 3. STM topographic image of (a) B-doped HOPG and (b) pure HOPG. Constant current mode with a scan rate of 30 Hz, sample bias of 100 mV, and tunneling current of 2 nA.

parison. Compared to the atomically flat surface of the undoped HOPG, the B-doped HOPG exhibits the hillocks on the originally smooth terrace, which is consistent with the observation in STM. However, compared with the STM image in Fig. 3(a), the hillock feature imaged by AFM in Fig. 4(a) is less significant. It is well established that, while the image contrast in AFM comes solely from the topography of the surface, one in STM arises from both the topography and the electronic density distribution. The more significant hillock feature in STM imaging of the B-doped HOPG indicates that the B doping perturbs not only the originally flat arrangement of the C atoms, but also the electronic structure of the graphite plane. The presence of the B atom, which lacks the  $p_z$  orbital, would significantly distort the otherwise well-ordered electronic structure of the graphite plane, which is composed of the  $p_z$  orbitals from the C atoms [17,18].

With regard to the structure of the B-doped HOPG, we can propose two possible models. First, the B atom can intercalate between the graphite planes. If this is the case, however, the XRD measurement of the B-doped HOPG should indicate the increased interlayer spacing because the trapped B atom would lead to weaker electronic interaction between the graphite planes. In addition, because the B atom is small enough to fit into the graphite planes [19], the flat topography of the graphite plane would not be affected by the intercalation of the B atom. Contrary to this prediction, our AFM result shows the topographic deformation of the graphite plane. Therefore, the intercalation model is not consistent with our results.

Another possibility is that the B atom substitutes a C atom in the graphite plane, as already proposed by several researchers [1–4,6–11]. The B atom, as a point defect in the graphite plane, would pull the neighboring

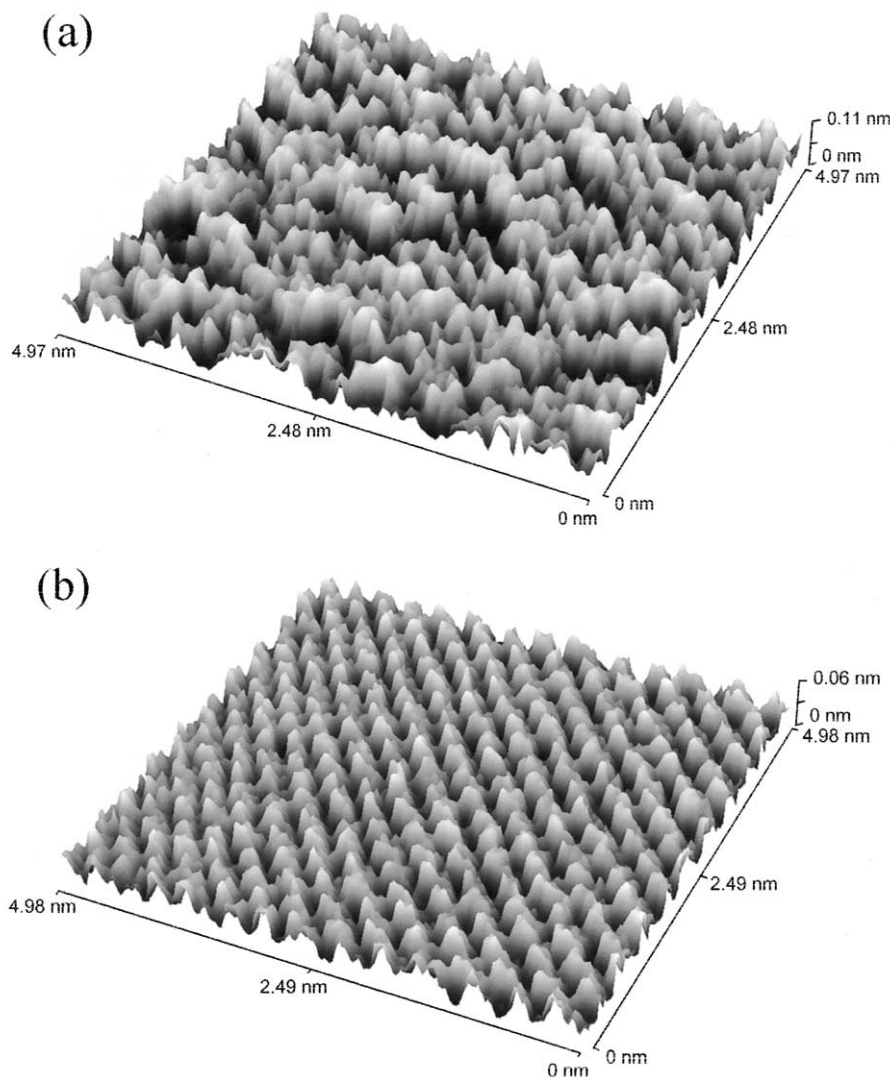


Fig. 4. AFM topographic image obtained from (a) the B-doped HOPG and (b) pure HOPG. The scan rate is 134 Hz with the force constant, 0.032 N/m.

C atoms and deforms the otherwise parallel C–C bonds. Moreover, the absence of  $p_z$  orbital in the B atom would make the  $p_z$  orbitals from the C atoms less conjugated, leading to the more disordered electronic structure.

#### 4. Conclusions

The boron-doped HOPG was characterized by X-ray photoelectron spectroscopy, XRD, and scanning probe techniques. The XPS measurement shows the slight shift of the C 1s peak to the lower binding energy, which is indicative of the C–B bond formation and the lowered density of  $\pi$  electron in the graphite planes. It is observed from the XRD measurements that the substituted B atom has no effect on the interlayer spacing of the graphite planes but makes the graphite plane less crystalline. The locally distorted structure of the B-substituted HOPG is revealed both by the scanning tunneling microscopy (STM) and by the AFM. It is shown that the substituted boron induces the electronic as well as the topographic distortion of the HOPG structure.

#### Acknowledgements

This work was funded by Samsung SDI. Also, this work was partially supported by the Brain Korea 21 Project in 2001 and the Korea Science and Engineering Foundation through the MICROS Center at KAIST.

#### References

- [1] C. Kim, Fujino, T. Hayashi, M. Endo, M.S. Dresselhaus, *J. Electrochem. Soc.* 147 (2000) 1265.
- [2] U. Tanaka, T. Sogabe, H. Sakagoshi, M. Ito, T. Tojo, *Carbon* 39 (2001) 931.
- [3] W. Cermignani, T.E. Paulson, C. Onneby, C.G. Pantano, *Carbon* 33 (1995) 367.
- [4] S. Jacques, A. Guette, X. Bourrat, F. Langlais, C. Guimon, C. Labrugere, *Carbon* 34 (1996) 1135.
- [5] T. Shirasaki, A. Derré, M. Ménétrier, A. Tressaud, S. Flandrois, *Carbon* 38 (2000) 1461.
- [6] M. Endo, C. Kim, T. Karaki, T. Tamaki, Y. Nishimura, M.J. Matthews, S.D.M. Brown, M.S. Dresselhaus, *Phys. Rev. B* 58 (1998) 8991.
- [7] M. Endo, C. Kim, K. Nishimura, T. Fujino, K. Miyashita, *Carbon* 38 (2000) 183.
- [8] C. Kim, T. Fujino, K. Miyashita, T. Hayashi, M. Endo, M.S. Dresselhaus, *J. Electrochem. Soc.* 147 (1999) 1257.
- [9] B.M. Way, J.R. Dahn, *J. Electrochem. Soc.* 141 (1994) 907.
- [10] C.E. Lowell, *J. Am. Ceram. Soc.* 50 (1967) 142.
- [11] B.M. Way, J.R. Dahn, T. Tiedje, K. Myrtle, M. Kasrai, *Phys. Rev. B* 46 (1992) 1697.
- [12] J.R. Dahn, J.N. Reimers, A.K. Sleight, T. Tiedje, *Phys. Rev. B* 45 (1992) 3773.
- [13] J.G. Naeni, B.M. Way, J.R. Dahn, J.C. Irwin, *Phys. Rev. B* 54 (1996) 144.
- [14] W.G. Zhang, H.M. Cheng, T.S. Xie, Z.H. Shen, B.L. Zhou, H.Q. Ye, *Carbon* 35 (1997) 1839.
- [15] G.P. Dai, T.S. Xie, H.M. Cheng, Y. Zhao, H.Q. Ye, *Carbon* 37 (1999) 994.
- [16] B.D. Cullity, in: *Elements of X-ray Diffraction*, Addison-Wesley, Reading, MA, 1978, p. 82.
- [17] J.R. Hahn, H. Kang, *Phys. Rev. B* 60 (1999) 6007.
- [18] J.R. Hahn, H. Kang, S. Song, I.C. Jeon, *Phys. Rev. B* 53 (1996) R1725.
- [19] A. John, in: *Dean Lange's Hand Book of Chemistry*, McGraw-Hill, New York, 1992, p. 4.13.
- [20] T. Shirasaki, A. Derré, K. Guérin, S. Flandrois, *Carbon* 37 (1999) 1961.
- [21] P.L. Walker, in: *Chemistry and Physics of Carbon*, vol. 7, Marcel Dekker, New York, 1971, p. 178.
- [22] J.F. Moulder, W.F. Stickle, P.E. Sobol, K.D. Bomben, *Handbook of X-ray Photoelectron Spectroscopy*, Physical Electronics, Perkin-Elmer, MN, 1994 (Chapter E).